Supplementary Material for

Tracking the spatiotemporal neural dynamics of object size and animacy in the human brain

Seyed-Mahdi Khaligh-Razavi[1], Radoslaw Martin Cichy[2],
Dimitrios Pantazis[3], and Aude Oliva[1]

1 Computer Science and Artificial Intelligence Laboratory,
Massachusetts Institute of Technology, Cambridge, Massachusetts, USA.
2 Department of Education and Psychology, Free University Berlin, Berlin, Germany
3 McGovern Institute for Brain Research,
Massachusetts Institute of Technology, Cambridge, Massachusetts, USA.

CORRESPONDING AUTHOR

Seyed-Mahdi Khaligh-Razavi
Current address:
Department of Brain and Cognitive Sciences,
Cell Science Research Center
Royan Institute for Stem Cell Biology and Technology
ACECR, Tehran, Iran

Phone: +1 857-285-1688
Email: skhaligh@mit.edu

37

Supplementary Table 1

39

| ROI	Left hemisphere		Right hemisphere	
	Onset latency	Peak latency	Onset latency	Peak latency
EVC	78 ±4	128 ±2	72 ±4	129 ±12
LO	85 ±10	148 ±40	86 ±14	148 ±32
TO	101 ±17	141 ±10	123 ±1	139 ±13
VO	107 ± 1	168 ±73	125 ±2	169 ±16
Fusi	112 ±2	173 ±112	133 ±3	164 ±34
PHC	119 ±10	173 ±20	123 ±1	172 ±15
ITG	160 ±1	173 ±95	121 ±4	142 ±50
MT	107 ±8	175 ±90	NA	144 ±229
IPS	160 ±23	173 ±108	135 ±2	142 ±115
SPL	114 ±13	181 ±242	88 ±4	260 ±263

40
41 **Supplementary Table 1: Onset and peak latencies for standard ROI-based MEG-fMRI**
42 **fusion results.** Values are obtained by 10000 bootstrap resampling of subjects. Values in
43 front of the ± indicate standard errors.

44
45
Supplementary Figure 1
47

A

B
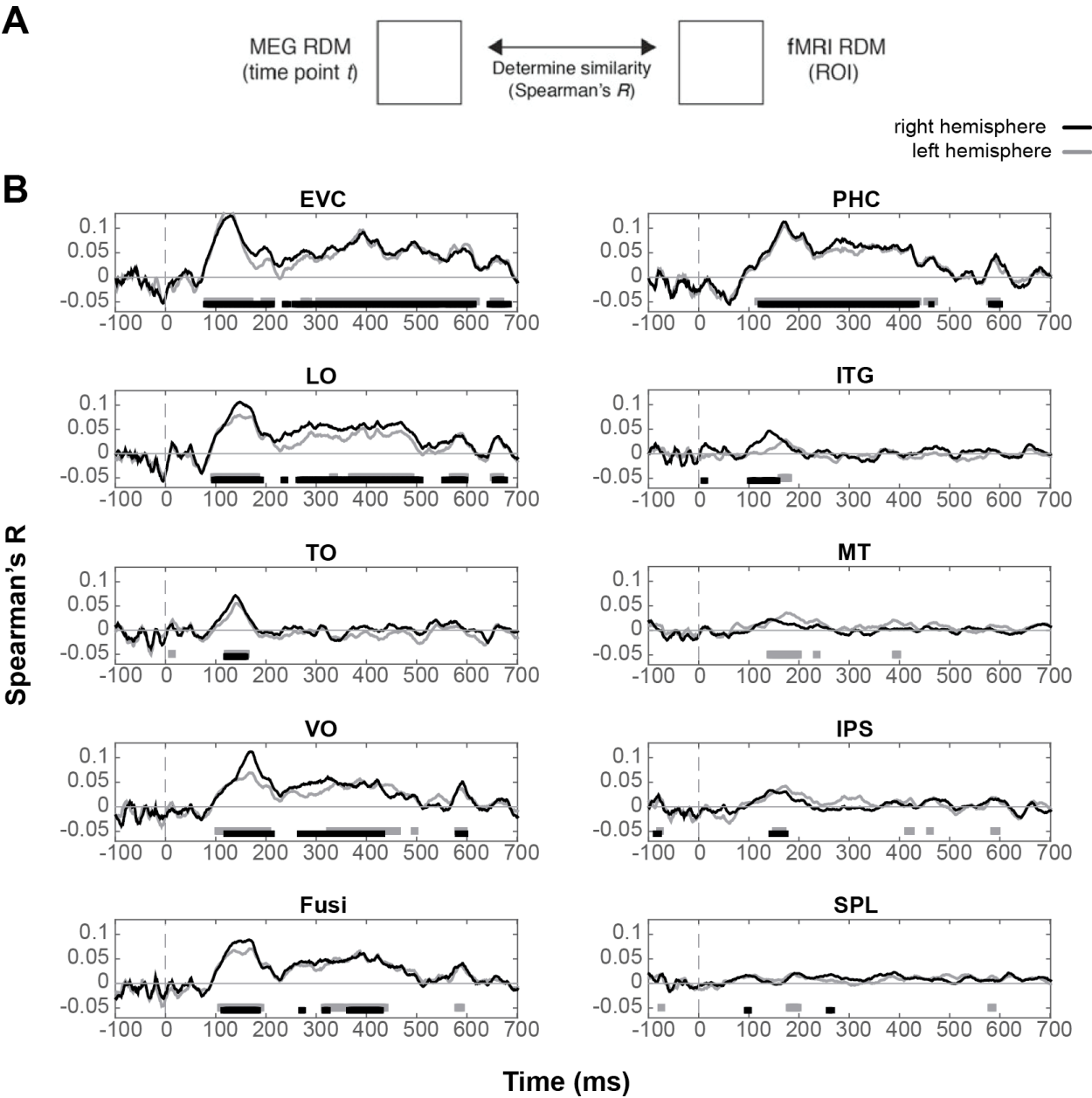
48
49
Supplementary Fig. 1. Standard ROI-based MEG-fMRI fusion. A) Method. For each ROI, we
correlated (Spearman's R) participant-specific fMRI RDM for each ROI with the average MEG-
RDM across subjects at each time point. This yielded a MEG-to-fMRI ROI time course for each
participant and time point. **B**) Results. The solid gray and black horizontal lines below time
courses show significant time-points (N = 15, one-sided sign-rank test, p < 0.05 FDR-corrected).
55
56
57
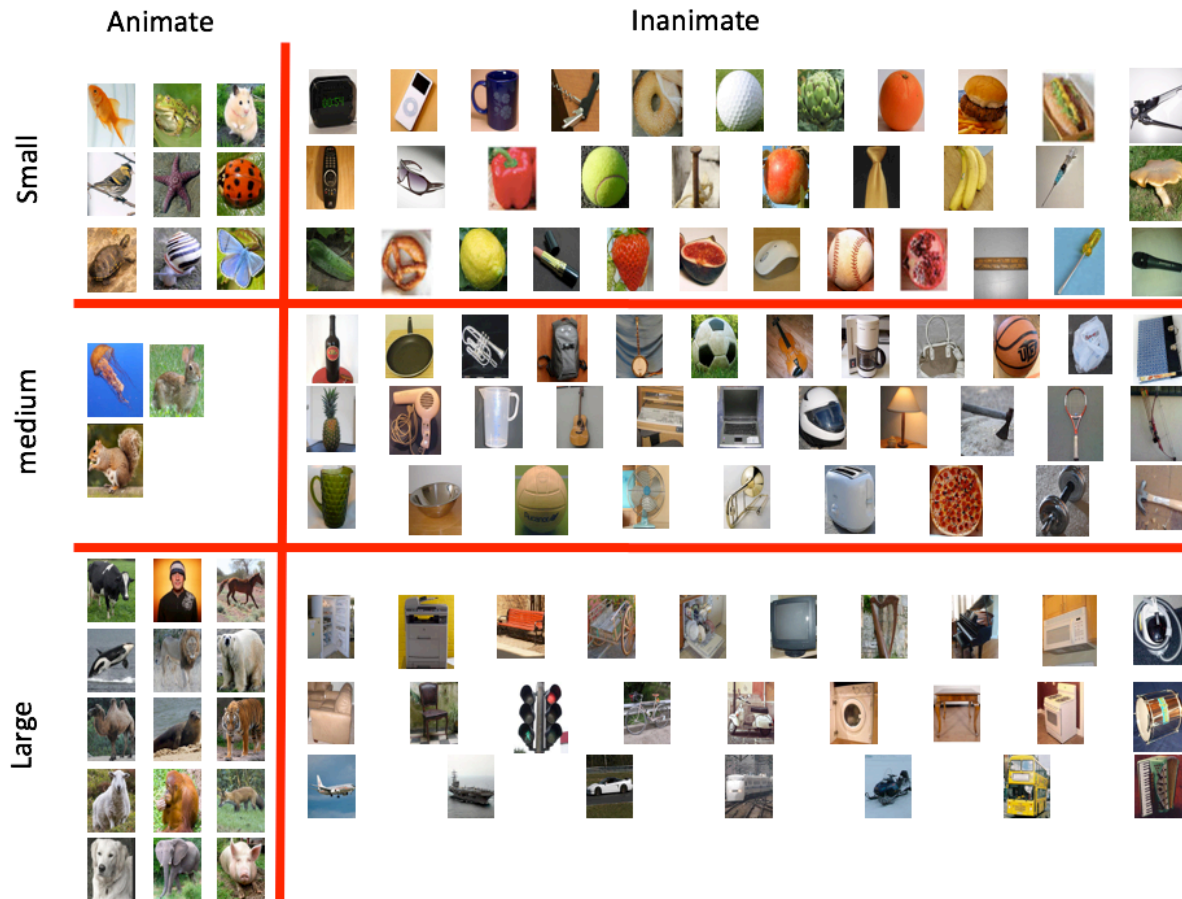
58
Supplementary Fig. 2. All stimuli divided by their animacy and real-world size. There were
118 images in total. The images were divided by their real-worlds size into three categories: 42
small sizes, 35 medium sizes, and 41 large sizes. The images were also divided by their
animacy: 27 animates, 91 inanimates.
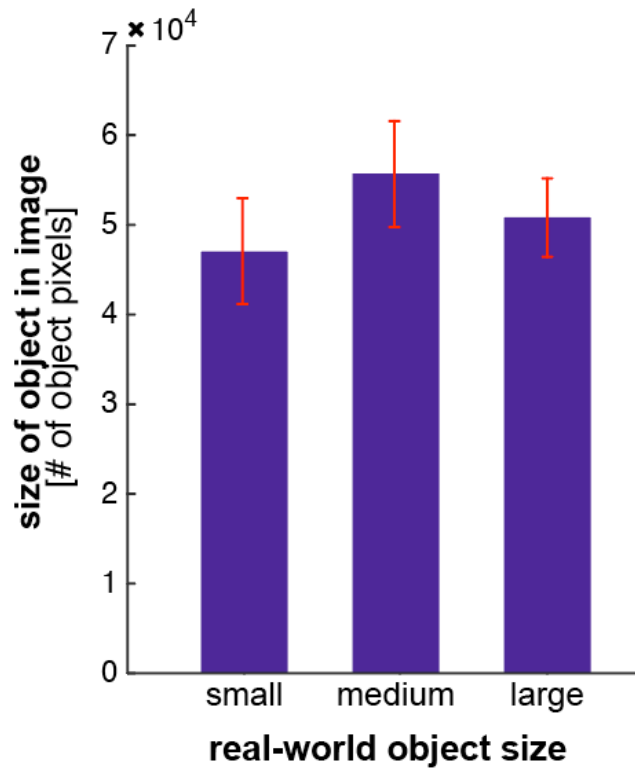
72
Supplementary Fig. 3. Distribution of the pixel-wise size of the 118 objects. We removed
the background from all the 118 images, and counted the number of non-background pixels
(object pixels) in each image. Bars show mean number of object pixels, and the error bars are
standard errors of the mean. None of the bars were significantly different from others [ANOVA,
$F(2,115) = 0.60$, $p = 0.547$; F-Crit=3.07].
78
79
80
81
82
83
84
85
86
87
88
89
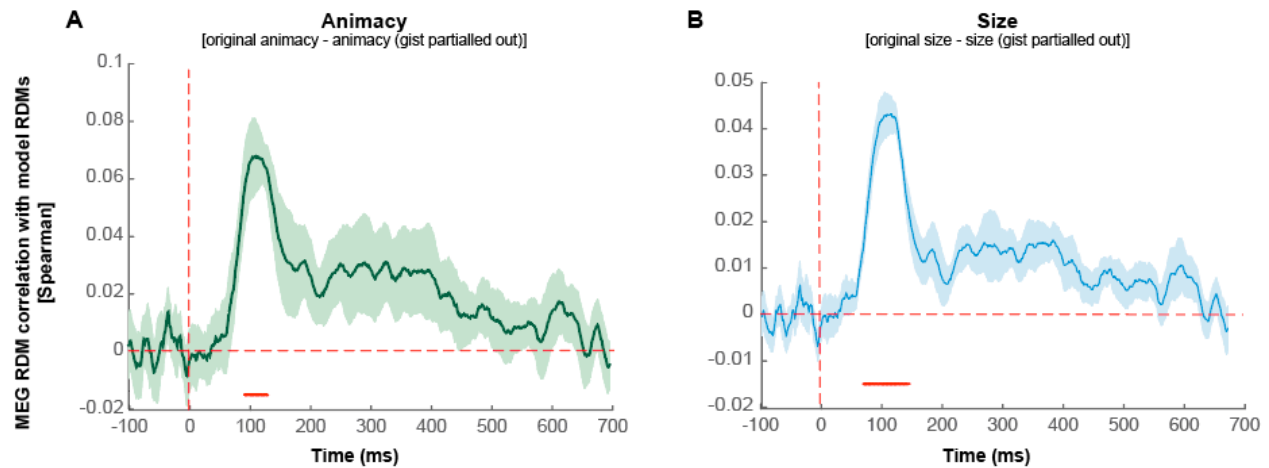
90
91 **Supplementary Fig. 4. The effect of regressing out low-level Gist visual features when**
92 **correlating A) animacy and B) size RDMs with MEG RDMs.** As in Fig. 5, we computed the
93 correlation of animacy/size RDMs respectively with MEG RDMs before and after regressing-out
94 the Gist model RDM. The red horizontal lines indicate time points with significant difference
95 between the original animacy/size correlation time-courses and the correlations after regressing
96 out the Gist RDM (two-sided signrank test, FDR-corrected at p = 0.05). There was a significant
97 difference only early between 93 and 130ms for animacy, and 79 to 150ms for size.
98